Non-affine dissipation in polymer fracture

Yazhuo Liu, Xianke Feng, Wei Hong *

Shenzhen Key Laboratory of Soft Mechanics & Smart Manufacturing, Department of Mechanics and Aerospace Engineering, Southern University of Science and Technology, Shenzhen, Guangdong 518055, China

A R T I C L E   I N F O

A B S T R A C T

Viscoelasticity is a universal property in most soft solids. Specifically, for the fracture of polymeric materials, viscoelasticity has often been regarded as a major mechanism of toughening, and the excess fracture energy beyond the intrinsic value correlated to the stress–strain hysteresis, which is commonly used to characterize viscoelasticity in the framework of continuum mechanics. Through systematically planned experiments, the current study shows that a noticeable package of energy dissipation exists besides that associated with the hysteretic deformation. This package of energy is attributed to the highly non-affine deformation near the crack tip — the rearrangement and mutual sliding of the neighboring chains caused by the rupture of a polymer chain, which are insignificant in samples under homogeneous deformation. Various means of inter-chain-friction reduction, e.g., by applying lateral stretches, diluting the chains with solvent, or subject the material to dynamic or static fatigue, can mitigate the effect of non-affine dissipation, and bring the fracture energy down to the intrinsic threshold. In contrast, by making an elastomer more elastic, e.g., by training through cyclic loading, the non-affine dissipation remains effective, and the limiting fracture energy is significantly higher than the threshold even when the hysteresis is negligible. The identification of the non-affine-dissipation mechanism paves the way to the development of new soft materials with both excellent elasticity and significant fracture toughness.

1. Introduction

Soft solids, such as elastomers and hydrogels, have found extensive uses in soft robotics[1,2], tissue engineering [3,4], flexible electronics [5,6], and other fields because of their low stiffness and high stretchability. Material fracture properties, which contribute to damage prediction and prevention, are crucial to most applications. In-depth researches have been carried out in related areas, including cutting [7–9], debonding [10], crack blunting [11], and theoretical prediction [12]. Among various mechanical properties, fracture energy and fatigue threshold have often been a center of focus in mechanics of soft solids. Fracture processes of solids are usually irreversible. Depending on the dissipation processes involved, the fracture energy, namely the work required to propagate a crack by unit area, is affected by various factors, such as the speed of crack propagation, temperature, and deformation history. On the other hand, the intrinsic fracture energy (or fatigue threshold), i.e. the minimum energy required for crack propagation, is usually believed to be a material parameter invariant with the state or history of deformation. In a rubbery polymer, the intrinsic fracture energy is the work required for a crack to propagate through a single layer of polymer chains in each loading cycle [13]. Analogous to the elastoplastic fracture of metals, the difference between the fracture energy Γ and intrinsic fracture energy Γ_0 has often been attributed to bulk viscous dissipation [14,15], which prevents the remote energetic driving force from being fully transmitted to the crack tip. Typically, the viscoelastic behavior of materials has an significant effect on the bulk energy dissipation [16]. Denoting the bulk dissipation as Γ_B, we can write the fracture energy as:

$$\Gamma = \Gamma_0 + \Gamma_B. \tag{1}$$

To measure the fracture properties of soft solids, various experiments are practiced [17], such as the pure shear test [18], the simple extension test [18], the single-edge crack test [19], and the trousers test [16]. Among them, the pure shear test is most often used to measure fracture energy, and the corresponding fatigue test [13] is often used to measure the fatigue threshold. During a pure shear test, as the crack propagates, a material particle in the process zone undergoes a loading–unloading process, as illustrated in Figs. 1(a) and 1(b). The stress–strain curves for loading and unloading of most soft elastomers and gels do not coincide, forming a hysteresis and dissipating energy. The bulk energy dissipation Γ_B is often attributed to the hysteresis [20] and it has been proposed that $\Gamma_B \propto h_{max}/(1 - h_{max})$, where
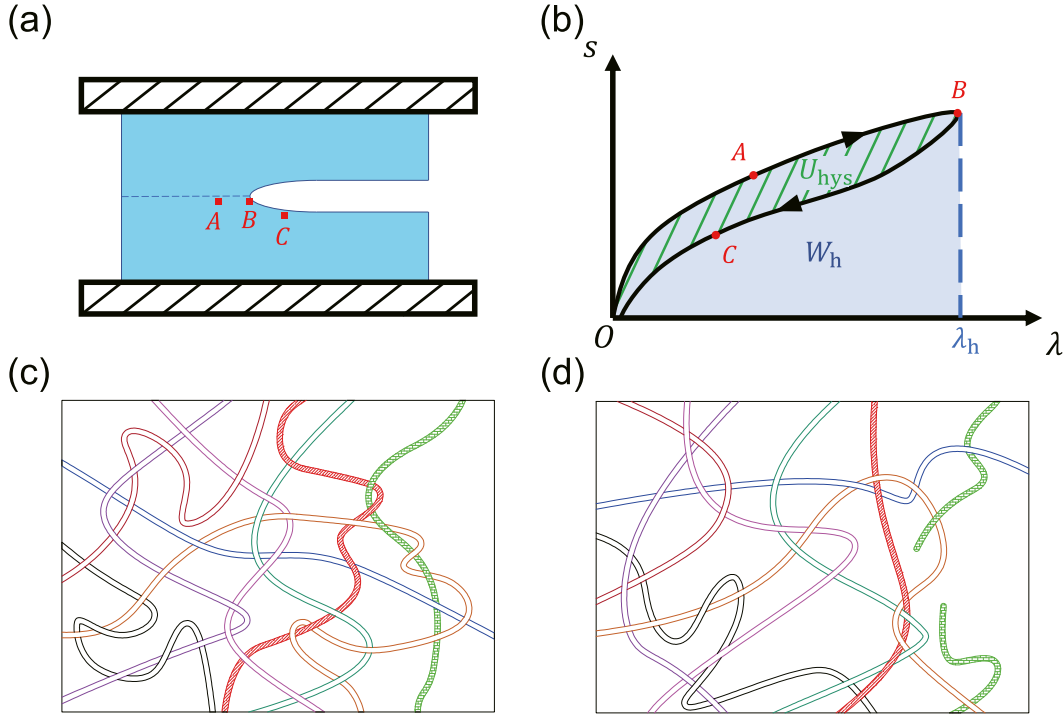
Fig. 1. (a) Schematic of crack propagation in a soft material subject to pure shear. Points A, B, and C represent the material particles in front of, on, and behind the crack tip, respectively. (b) Schematics of the loading and unloading stress–stretch curves of a sample stretched to λ_h, close to the stretch limit λ_{max}. The states of the three material particles in (a) are marked on the curves accordingly . The work of stretching W_h is the area below the loading curve, and the energy dissipation U_{hys} is the area enclosed between the loading and unloading curves. (c) Schematic of a polymer-chain bundle at the crack tip before crack propagation. The green polymer chain is the next to break. (d) The same bundle after the crack propagates by a single chain. The next chain (red) is now straightened. Mutual sliding occurs among polymer chains in the cluster during the rearrangement of relative location and redistribution of load. (For interpretation of the references to color in this figure legend, the reader is referred to the web version of this article.)

h_{max} is the ratio between the hysteresis U_{hys} and the work of stretching W_h, at the maximum stretch prior to rupture, $h_{max} = U_{hys}/W_h$. Based on this assumption, various theories and models have been developed to predict fracture energies in different circumstances [12,21]. Furthermore, it has also been observed that prior deformation history along the loading direction can reduce fracture energy [12,21]. The present study seeks to further unveil the mystic relations among these energy packages. Most elastomers exhibit the Mullins effect − the unloading curve does not coincide with the loading curve, exhibiting a hysteresis. For these elastomers, training (i.e., stretching along the loading direction and then releasing) can help to reduce hysteresis due to the irreversible softening. When the training stretch approaches the tensile limit of the elastomer, the hysteresis of the material is minimized − in other words, the continuum deformation of the elastomer is almost fully elastic. If the bulk dissipation Γ_B came entirely from the hysteresis, the fracture energy of the fully trained elastomer should have approached the threshold Γ_0 in this limiting case. Nevertheless, the experiments here follow show that although the fracture energy is reduced after training, the limit is still much larger than the fatigue threshold.

To resolve this discrepancy and to identify the missing energy package, let us re-examine the basic assumptions. The hysteresis of the stress–strain curve is measured from a sample undergoing homogeneous deformation, and its applicability relies on the validity of the continuum assumption − that one can always subdivide a deforming body into small elements, in which the deformation is virtually uniform. However, the singularity at the crack tip can give rise to a huge strain gradient locally. With the characteristic size comparable to the mesh size of a polymer chain length, the classic continuum assumption may breakdown [22,23], and the hysteresis obtained from uniform deformation may not be applicable to the crack tip. At this length scale, the

rupture of one polymer chain will cause load redistribution to the surrounding chains, thereby changing the local chain config- uration and bringing inter-chain sliding which dissipates energy, as illustrated by Figs. 1(c) and 1(d). Recent experiments [24–26] visualizing the local damage due to bond scission which only occurs at the tip of a propagating crack, and is not present in bulk deformation, provide evidence for the proposed mechanism. Since the deformation involving mutual sliding is highly non- affine, we will thus refer to the energy dissipation associated with such a process as non-affine dissipation (NAD).

2. Elastic limit and fatigue threshold

To clarify the effect of hysteresis on bulk energy dissipation, we carried out a series of experiments by using the Ecoflex 00-30 (Smooth-On, Inc.) silicone rubber as a model system. We mixed the A and B components at a mass ratio of 1:1, degassed the mixture in a vacuum chamber, casted it in an acrylic mold, and then left it in a 65 °C environmental chamber for 4 h. For all experiments except the fatigue test, the nominal strain rate was fixed at $\dot{\lambda} = 0.1\ s^{-1}$ and the loading amplitude was reported in terms of the energy release rate. All energy release rates and fracture energies were measured through pure shear tests on pre- notched samples of size $40 \times 25 \times 2$ mm [3] (width $\times$ height $\times$ thickness), and pre-cut edge cracks of length $\sim$10 mm, as sketched in Fig. 1(a).

From the uniaxial tension test, we measured the loading and unloading stress–strain curves of our samples and plotted them in Fig. 2(a). The Mullins effect of our sample was also verified by loading and unloading the sample with increasing maximum stretch, as shown in Fig. 2(b). Lake and Thomas provided an estimate of the intrinsic fracture energy [13]
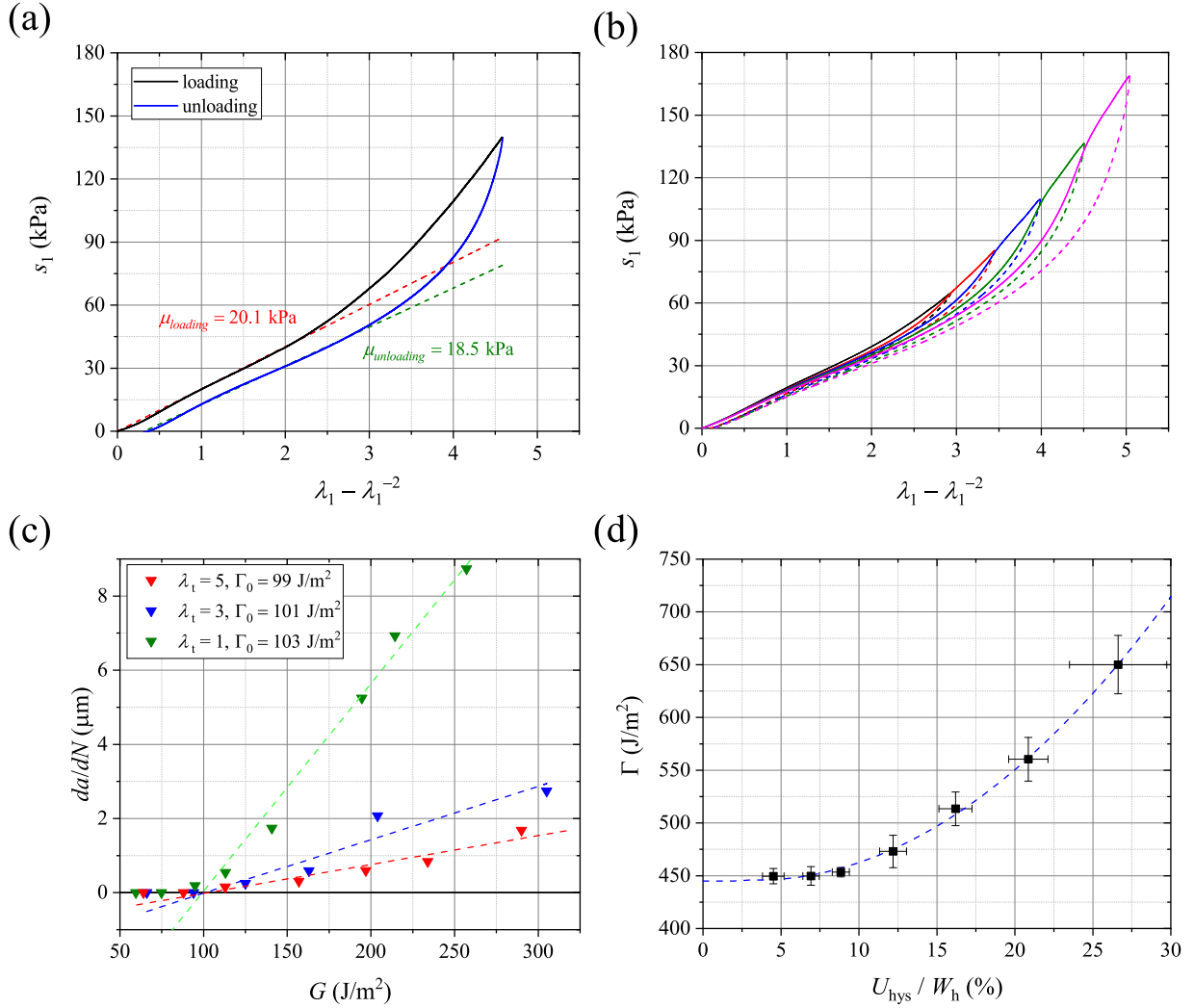
$$\Gamma_0 \sim \frac{U}{\Omega} l \sqrt{n}, \tag{2}$$

Fig. 2. (a) Nominal stress vs. the reduced stretch of Ecoflex 00-30 measured from uniaxial tension. The shear modulus is 20.1 kPa during loading and 18.5 kPa for unloading. (b) Mullins effect of Ecoflex 00-30. The solid and dash lines represent the loading and unloading processes, respectively. (c) Crack growth per cycle as a function of energy release rate after different training stretches λ_t. Γ_0 in the legend is the fatigue threshold obtained in each case. (d) Fracture energy as a function of hysteresis. The relative hysteresis U_{hys}/W_h is gradually reduced by training the material through increasingly larger stretch.

where U is the energy required to break a covalent bond (i.e., a link connecting two monomers), l is the length of a link, n is the number of links per chain and Ω is the effective volume occupied by each monomer. For silicone rubber, a polymer chain is ruptured by breaking either a silicon–silicon bond or a silicon–oxygen bond. The averaged bond energy of these bonds is estimated as $U \approx 7.0 \times 10^{-19}$ J. The monomer volume is $\Omega \approx 1.0 \times 10^{-28}$ m³, and the link length $l \sim \sqrt[3]{\Omega} \approx 0.5$ nm. The number of links per chain n can be calculated as $n = (N\Omega)^{-1}$ from the chain density N, which in turn can be estimated from the initial shear modulus

$$\mu = NkT. \tag{3}$$

We take the measured shear modulus $\mu = 20.1$ kPa, and the product between the Boltzmann constant and temperature $kT \approx 4.1 \times 10^{-21}$ J at room temperature. Substituting all parameters back into (2), we estimate the intrinsic fracture energy $\Gamma_0 \sim Ul\sqrt{n}/\Omega \approx 146.7$ J/m², which agrees fairly well with the measured threshold $\Gamma_0 \sim 100$ J/m² as shown by Fig. 2(c), despite the coarse estimation. It is noteworthy that the value of n and thus the threshold Γ_0 could be overestimated due to the presence of defects or dangling chains in the polymer network. Fig. 2(d) plots the fracture energy Γ as a function of the hysteresis dissipation

U_{hys}. The hysteresis is reduced to different levels by training the material to different maximum stretches and is measured by loading the sample to a maximum stretch $\lambda = 5$ then unloading it. A plateau appears where hysteresis is close to 0 — the elastic limit Γ_T emerges. Generally, the elastic limit Γ_T is not a material constant and may depend on loading rate, fracture mode, etc. As discussed previously, if the bulk dissipation Γ_B in Eq. (1) is a direct consequence of the hysteresis, the elastic limit Γ_T should be close, if not equal, to the fatigue threshold Γ_0. However, for the material tested, the elastic limit is conspicuously higher than the fatigue threshold, which suggests other means of dissipation. This new package of energy dissipation is not captured by the hysteresis of a sample subject to homogeneous deformation of nearly affine polymer network, and is likely to be linked to some process which takes place when a crack is present. It is noteworthy that, due to the flaw-tolerance and exceptional stretchability of Eco-flex, the samples could be stretched to the limit of homogeneous deformation which is close to the maximum stretch near the crack tip, so that the contribution from bulk viscoelastic dissipation could be minimized, and that from NAD clearly identified. The presence of the plateau corresponding to the elastic limit on Fig. 2d is another evidence of this limit. In other less stretchable materials, of which the limit is hardly reachable in homogeneous deformation, the

isolation of NAD contribution from bulk viscoelastic dissipation may not be as easy.

A possible microscopic process is speculated as follows to understand the microscopic picture of NAD. Imagine a bundle of polymer chains in different directions at the crack tip as sketched in Fig. 1(c). For clarity, we assume the polymer network to be fully elastic when subject to homogeneous deformation and neglect the contributions from entanglements or other physical crosslinks. Prior to crack propagation, the shared load on each polymer chain gradually increases. In a quasi-static case, the chain configuration and load distribution minimize the free energy of the system. When the crack extends by a minimal amount by breaking one polymer chain in the bundle, the classic Lake-Thomas picture envisions that the energy stored in all links of this chain is irreversibly released [13], contributing to the fatigue threshold Γ_0. However, due to the intertwining topology of the polymer chains, such a process is not to be completed without affecting others in the bundle. To reach a local equilibrium, the load originally carried by the broken chain is redistributed among the remaining polymer chains, another chain in the neighborhood may be straightened, and the bundle is reconfigured as illustrated by Fig. 1(d), with inevitable inter-chain sliding. The reconfiguration of the chain bundle is by no means affine. Such a process is repeated continuously during the crack propagation, accompanied by the constant reconfiguration of the chain bundle at the then-current crack tip.

The mutual sliding during chain reconfiguration contributes significantly to the fracture energy. The NAD occurs in a process zone near the crack tip, with its size comparable to the length of a polymer chain. The NAD is only seen at crack propagation, when the polymer chains rupture sequentially, so that the mutual sliding can be manifested. In a process of homogeneous deformation, the polymer network is nearly affine, and the effect of mutual sliding is minimal. On the other hand, a different scenario can be envisioned when a polymer network is subject to fatigue loading. Even when the peak load is not enough to break a polymer chain and overcome the NAD for chain rearrangement at the same time, the subsequent cyclic loading would ultimately accumulate enough energy to rearrange the chains for the next breakage. Therefore, the NAD does not contribute to the fatigue threshold, which is identical to the intrinsic fracture energy Γ_0 of the material.

3. A universal threshold

Based the underlying mechanism of NAD, if one can design proper procedures to reduce or avoid the sliding between polymer chains, the fracture energy will be reduced and ultimately approach the intrinsic fracture energy Γ_0, which is a true material parameter and a universal threshold for all fracture processes of rubbery polymers. To further verify the hypothesis, we performed a series of procedures to reduce chain sliding or NAD, and systematically studied their effects on fracture.

As the NAD involves the mutual sliding among polymer chains, especially those in different directions, one could imagine that straightening the transverse chains by applying a lateral pre-stretch may reduce the effect. Therefore, it is expected that the fracture energy should decrease with the lateral pre-stretch. If sufficient pre-stretch is applied laterally, the mutual sliding between polymer chains can be avoided and the fracture energy approaches the threshold Γ_0. To test this hypothesis, we carry out pure shear tests to a series of laterally pre-stretched samples. We applied horizontal stretches of different values, λ_{pre}, to identical samples of Ecoflex 00-30, held by clamping the top and bottom edges with rigid acrylic bars, as illustrated in Fig. 3(a), and then loaded individually in the vertical direction through the acrylic

bars. The fracture tests were carried out over samples which were pre-stretched and clamped in the same way, but prepared with pre-existing edge cracks. The fracture energies are then calculated by integrating the stress–stretch curves of the pre-stretched samples without pre-crack, up to the critical displacement at which the pre-cracked one ruptured, to evaluate the excess strain energy density $W_c\left(\lambda_{pre}\right)$, and then dividing it by the original height H of the non-cracked sample prior to pre-stretch.

$$\Gamma\left(\lambda_{pre}\right) = W_c\left(\lambda_{pre}, \lambda_c\right)/H. \tag{4}$$

The stored strain energy due to lateral prestretch is excluded from W_c and subsequently from Γ, as the material behind the crack tip would still be subject to the same lateral stretch and this part of elastic energy will not be released after crack propagation. The original geometry prior to prestretch is used so that a fair comparison could be made between the measured fracture energies of the prestretched samples and the threshold measured without prestretch.
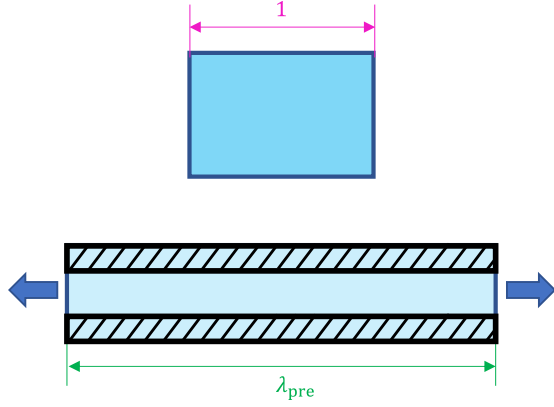
By computing the fracture energy with reference to the cross-sectional geometry prior to the lateral pre-stretch, we plot the measured fracture energy as a function of the pre-stretch in Fig. 3(b). As expected, the fracture energy Γ decreases monotonically with the lateral pre-stretch λ_{pre}, and quickly approaches the fatigue threshold Γ_0. As a reference, we also measured the relative hysteresis U_{hys}/W_h of the non-cracked samples subject to axial loads, and plot it against the lateral pre-stretch. As expected, the lateral stretch reduces the hysteresis of axial loads, but the relatively small reduction in hysteresis could never account for the large decrease in fracture energy. Unlike the training stretch which reduces the homogeneous viscoelasticity hysteresis without avoiding mutual chain sliding, the lateral pre-stretch reduces both bulk viscoelastic dissipation and NAD.

Aside from separating the lateral chains via mechanical pre-stretch, it is natural to expect that a swelling process, which inserts small solvent molecules amongst the polymer chains, may lubricate the mutual sliding and thus reduce the NAD. Due to the smaller size of the solvent molecules, their viscosity is expected to be much lower than that of the dry polymer, and thus the energy dissipation due to inter-chain sliding could be significantly reduced. The reduction is expected to be more significant at higher swelling ratios, when the polymer chains are further separated by solvent molecules. By minimizing interchain sliding, the swelling process reduces both the NAD and the bulk viscosity associated with affine deformation. Therefore, it is expected that the fracture energy of the material decreases with the swelling ratio, approaching the fatigue threshold.
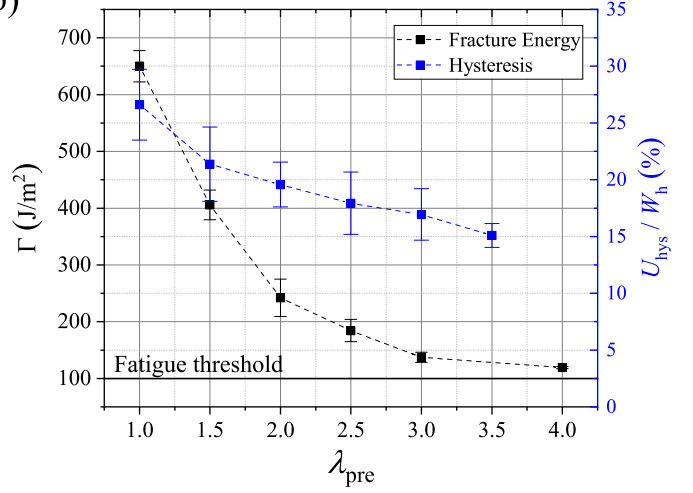
To test the effect of swelling on the NAD, we prepared the samples by immersing the as-cured Ecoflex 00-30 films in dodecane (CAS No. 112-40-3) for various durations, and then leaving them in sealed bags to homogenize the solvent distribution. Dodecane was selected for sufficient swelling and insignificant evaporation during the tests. The swollen samples were then subject to pure shear tests, and the resulting nominal fracture energies are shown in Fig. 3(d), against the volumetric swelling ratio. For better comparison, the fracture energy was calculated with respect to the geometry before swelling. Just as expected, as the swelling ratio increases, the fracture energy of the sample gradually decreases, approaching almost the same threshold as in the fatigue and pre-stretch tests.

It has already been shown that the fatigue threshold is unaffected by the NAD. Analogously, it is natural to wonder whether a static fatigue process will be affected by NAD or will it follow the same threshold. During a static fatigue process, the sample is held at constant displacement. Although there is no external cyclic load to shake the polymer bundle through the rearrangement process, the thermal fluctuation will also cause the polymer
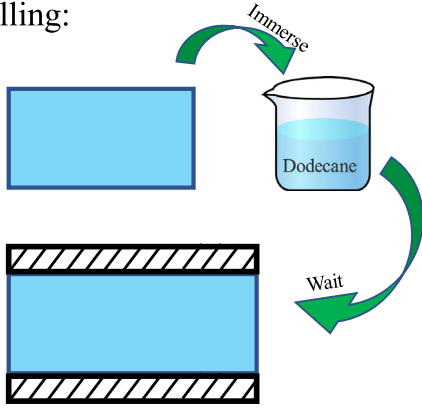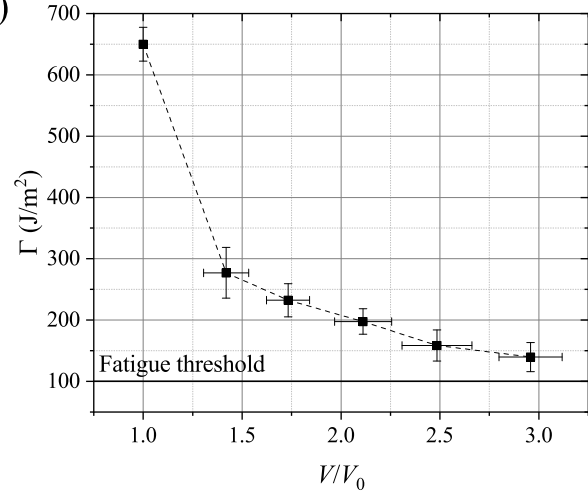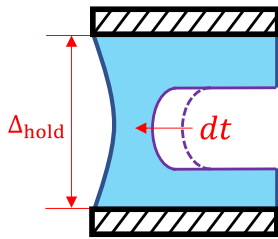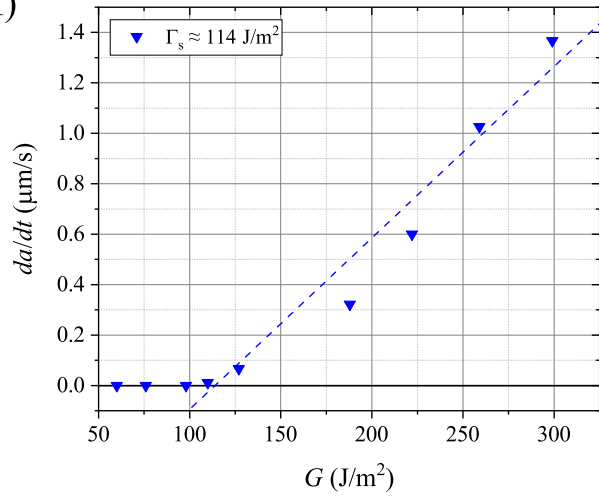
Fig. 3. (a) Schematic of lateral pre-stretch. Each sample was stretched to λ_{pre} and then held by rigid acrylic bars before testing. (b) Fracture energy and hysteresis ratio of Ecoflex 00-30 as a functions of the lateral pre-stretch. (c) Schematic of the swelling process. The as-cured sample was immersed in dodecane for a certain time, sealed in a package to equilibrate, and then clamped between acrylic bars for testing. (d) Fracture energy of Ecoflex 00-30 as a function of the volume swelling ratio. The static fatigue threshold of Fatigue threshold $\Gamma_0 = 100$ J/m^2 is shown in (b) and (d) as a reference. The error bars indicate the range of data. (e) Schematic of the static fatigue test. The crack extension da was measured over the undeformed state. (f) Speed of crack propagation as a function of the energy release rate. A threshold $\Gamma_s \approx 114$ J/m^2 was observed.
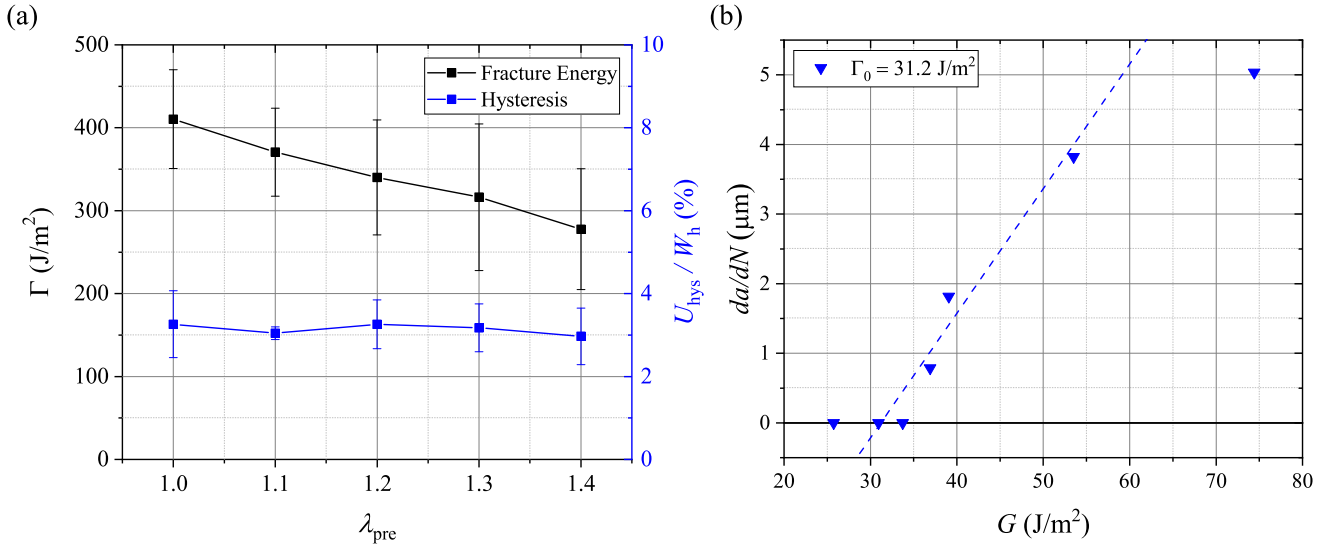
(a)

(b)

Fig. 4. (a) Fracture energy and hysteresis ratio of PDMS samples as functions of the lateral pre-stretch. The error bars indicate the range of data. (b) Results of fatigue tests on the PDMS samples: the crack extension rate as a function of the applied energy release rate. A fatigue threshold $\Gamma_0 \approx 31.2$ J/m^2 is identified.

chains to gradually experience every possible configuration, until the state for the breakage of the next chain is reached. Therefore, the NAD does not affect the static fatigue, whose threshold should be the same universal threshold Γ_0. Here, we carried out a series of static fatigue tests by loading pre-cracked Ecoflex 00-30 samples to and then holding at certain stretches while measuring the speed of crack propagation under an optical microscope, as sketched in Fig. 3(e). The resulting crack speed is plotted as a function of the applied energy release rate in Fig. 3(f), and a threshold of $\Gamma_s \approx 114$ J/m^2 can be identified. Just as expected, the static fatigue threshold is also reasonably close to the universal threshold Γ_0.

4. Other material systems

In all experiments presented in prior sections, we used Ecoflex 00-30 as a sample system to show the effects of the NAD and the universality of the fatigue threshold Γ_0. However, these phenomena and the underlying mechanisms are never limited to this material. Instead, it is expected that similar behaviors shall be observed in all rubbery polymers. To demonstrate the universality, we carried out additional tests on a polydimethylsiloxane (PDMS, SYLGARD 184). The samples were prepared by mixing at a weight ratio of A:B = 30:1, degassing, casting in a glass mold, and then resting in a 65 °C environment chamber for 24 h. The cured samples were demolded and tested at room temperature.

A batch of notched PDMS samples were pre-stretched and held laterally at different stretches, and then subject to pure shear tests to measure the fracture energy Γ. Another batch of unnotched samples were also pre-stretched to the same lateral stretches, and then subject to uniaxial tension up to $\lambda_h = 1.4$ to measure the hysteresis. Both data are plotted in Fig. 4(a) as functions of the lateral pre-stretch λ_{pre}. In the meanwhile, fatigue tests were carried out on a set of identical PDMS samples, with the results shown on Fig. 4(b). As can be read from Fig. 4(a), being a quite elastic material, the PDMS exhibited a relatively low hysteresis, hardly affected by the pre-stretch. On the other hand, the pre-stretch gradually brought the fracture energy down by ~30%. Compared to the Eco-flex 00-30 material system, the PDMS samples are more complex. The components ratio was modified from the recommended 10:1 to 30:1 in order to soften the sample to allow lateral pre-stretch. However,

the high monomer-crosslinker ratio leads to extraordinary long polymer chain lengths, which makes the lateral pre-stretch less effective on reducing the mutual sliding as well as NAD. On the other hand, the relative brittleness of PDMS only allowed a lateral pre-stretch of no larger than 1.4, which was far less than that in the Eco-flex experiments. The large gap between the minimum fracture energy and the fatigue threshold, as shown by Fig. 4, could possibly be attributed to the relatively low pre-stretch, which hardly unraveled the chain bundles at the crack tip for effective NAD reduction. Although the effect is weakened, the observation that the fracture energy was uncorrelated with the hysteresis, again demonstrated the physical significance of NAD and exemplified its contribution to the fracture energy.

Highly swollen in a low viscosity solvent, water, hydrogels serve as another good example for the mechanism discussed here. However, the polymers for most hydrogels are glassy when dry, preventing a direct comparison to be made to the dry state. Here, we take the lowest water content state as a reference, assume PAAm hydrogels have the same density with water, and then reexamine the published data on the swelling dependence of the fracture and fatigue properties of a Polyacrylamide (PAAm) hydrogels in the literature [27]. Due to the low viscosity and high volume fraction of water, it is expected that the polymer chains in a swollen hydrogel are widely separated by water molecules, and the apparent viscosity of a hydrogel is close to that of water, less dependent on the swelling ratio. The fact that the fracture energy reduces significantly at high water concentrations serves as another evidence of the role of NAD. It can be seen that, even for the highly swollen gel, its fracture energy is still much higher than the threshold. The discrepancy suggests that, unlike the solvent-dominated bulk viscosity, the NAD has not been fully eliminated at this swelling ratio (~4 × volumetric), as the polymer in other directions may not have been straightened or disentangled from the broken one at the crack tip (see Fig. 5).

5. Conclusion

For the fracture of rubbery elastomers, a noticeable gap exists between the elastic limit of fracture energy and the fatigue threshold embodies a distinct package of energy, suggesting a dissipation mechanism that cannot be ascribed to the stress–strain
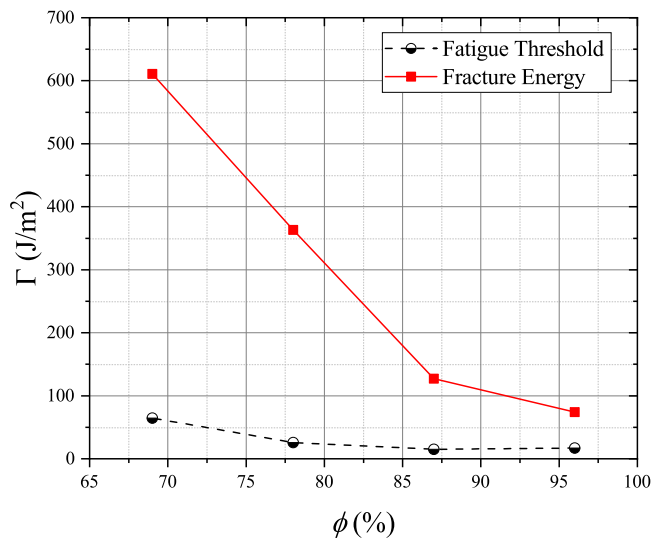
Fig. 5. Nominal fracture energy and fatigue threshold of PAAm hydrogel as functions of water mass fraction ϕ. The values are calculated by multiplying the measured value by the area swelling ratio relative to the reference (the one of lowest water fraction). (Recalculated from the experimental data in Ref. [27].).

hysteresis loop under uniform deformation. Theory of elasticity suggests high stress concentration and large strain gradient at the vicinity of a crack tip, where the applicability of classical continuum assumption becomes questionable. Furthermore, within the fracture process zone, multiple polymer chains are highly entangled and constantly interacting with each other, thus a macroscopic strain cannot even be defined. In this letter, by considering the configurational change and mutual sliding among the surrounding polymer chains when a single polymer chain breaks, we propose a microscopic energy-dissipation mechanism associated with the non-affine deformation at the crack tip. Such a NAD mechanism is effective only when a crack propagates at a finite rate, otherwise the presence of thermal fluctuation can always bring the chains to the configuration for the next rupture event.

To verify such a mechanism, we carried out a series of fracture and fatigue tests on Ecoflex silicon rubber, about the effects of various factors, including lateral pre-stretches, swelling by solvent, and static and dynamic fatigue. A universal threshold was identified in dynamic and static fatigue tests, as well as the fracture energies of highly swollen samples or laterally pre-stretched samples, and the measured value agreed well with that estimated from the Lake–Thomas model. This universal threshold represents the minimum energetic driving force for crack propagation, namely, the intrinsic fracture energy. On the other hand, when the same material was trained with sufficient cyclic loading to minimize the hysteresis on stress–strain curves, the limiting fracture energy is significantly higher than the threshold, suggesting the contribution of NAD in polymer networks. Experiments on other material systems further verify the universality of the proposed NAD mechanism.

Hopefully, the distinction between the NAD from viscoelastic dissipation through affine deformation may inspire future design of elastomeric materials that are highly elastic yet tough against fracture. These materials have foreseeable applications in scenarios when minimum hysteresis is desired in working conditions, and fault tolerance and reliability are also of concern.

Declaration of competing interest

The authors declare that they have no known competing financial interests or personal relationships that could have appeared to influence the work reported in this paper.

Data availability

Data will be made available on request.

Acknowledgments

References

[1] R.V. Martinez, et al., Robotic tentacles with three-dimensional mobility based on flexible elastomers, Adv. Mater. 25 (2) (2013) 205–212.

[2] Z. Suo, Mechanics of stretchable electronics and soft machines, MRS Bull. 37 (2012) 218–225, http://dx.doi.org/10.1557/mrs.2012.32.

[3] K.T. Nguyen, J.L. West, Photopolymerizable hydrogels for tissue engineering applications, Biomaterials 23 (2002) 4307–4314, http://dx.doi.org/10.1016/S0142-9612(02)00175-8.

[4] K.Y. Lee, D.J. Mooney, Hydrogels for tissue engineering, Chem. Rev. 101 (2001) 1869–1880, http://dx.doi.org/10.1021/cr000108x.

[5] Y. Li, W. Liu, Y. Deng, W. Hong, H. Yu, Miura-ori enabled stretchable circuit boards, Npj Flex. Electron. 5 (2021) 3, http://dx.doi.org/10.1038/s41528-021-00099-8.

[6] Jeong G.S. others, Solderable and electroplatable flexible electronic circuit on a porous stretchable elastomer, Nature Commun. 3 (2012) 977, http://dx.doi.org/10.1038/ncomms1980.

[7] Y. Liu, C.-Y. Hui, W. Hong, A clean cut, Extreme Mech. Lett. 46 (2021) 101343, http://dx.doi.org/10.1016/j.eml.2021.101343.

[8] E. Reyssat, T. Tallinen, M. Le Merrer, L. Mahadevan, Slicing softly with shear, Phys. Rev. Lett. 109 (2012) 244301, http://dx.doi.org/10.1103/PhysRevLett.109.244301.

[9] A. Spagnoli, R. Brighenti, M. Terzano, F. Artoni, Cutting resistance of soft materials: Effects of blade inclination and friction, Theor. Appl. Fract. Mech. 101 (2019) 200–206, http://dx.doi.org/10.1016/j.tafmec.2019.02.017.

[10] C. Creton, J. Hooker, K.R. Shull, Bulk and interfacial contributions to the debonding mechanisms of soft adhesives: Extension to large strains, Langmuir 17 (2001) 4948–4954, http://dx.doi.org/10.1021/la010117g.

[11] C.Y. Hui, A. Jagota, S.J. Bennison, J.D. Londono, Crack blunting and the strength of soft elastic solids, Proc. Math. Phys. Eng. 459 (2003) 1489–1516.

[12] T. Zhang, S. Lin, H. Yuk, X. Zhao, Predicting fracture energies and crack-tip fields of soft tough materials, Extreme Mech. Lett. 4 (2015) 1–8.

[13] G.J. Lake, A.G. Thomas, The strength of highly elastic materials, Proc. R. Soc. Lond. Ser. A Math. Phys. Eng. Sci. 300 (1967) 108–119.

[14] X. Zhao, Multi-scale multi-mechanism design of tough hydrogels: Building dissipation into stretchy networks, Soft Matter 10 (2014) 672–687, http://dx.doi.org/10.1039/c3sm52272e.

[15] C. Creton, M. Ciccotti, Fracture and adhesion of soft materials: a review, Rep. Progr. Phys. 79 (2016) 046601, http://dx.doi.org/10.1088/0034-4885/79/4/046601.

[16] Gent, A. N, Adhesion and strength of viscoelastic solids. Is there a relationship between adhesion and bulk properties? Langmuir 12 (1996) 4492–4496, http://dx.doi.org/10.1021/la950887q.

[17] R. Long, C.-Y. Hui, Fracture toughness of hydrogels: measurement and interpretation, Soft Matter 12 (2016) 8069–8086, http://dx.doi.org/10.1039/C6SM01694D.

[18] R.S. Rivlin, A.G. Thomas, Rupture of rubber. I. Characteristic energy for tearing, J. Polym. Sci. 10 (1953) 291–318, http://dx.doi.org/10.1002/pol.1953.120100303.

[19] Greensmith H. W., Rupture of rubber. X. The change in stored energy on making a small cut in a test piece held in simple extension, J. Appl. Polym. Sci. 7 (1963) 993–1002, http://dx.doi.org/10.1002/app.1963.070070316.

[20] A.G. Evans, Z.B. Ahmad, D.G. Gilbert, P.W.R. Beaumont, Mechanisms of toughening in rubber toughened polymers, Acta Metall. 34 (1986) 79–87, http://dx.doi.org/10.1016/0001-6160(86)90234-8.

[21] Y. Qi, J. Caillard, R. Long, Fracture toughness of soft materials with rate-independent hysteresis, J. Mech. Phys. Solids 118 (2018) 341–364.

[22] D.C.C. Lam, F. Yang, A.C.M. Chong, J. Wang, P. Tong, Experiments and theory in strain gradient elasticity, J. Mech. Phys. Solids 51 (2003) 1477–1508, http://dx.doi.org/10.1016/S0022-5096(03)00053-X.

[23] H. Gao, Y. Huang, W.D. Nix, J.W. Hutchinson, Mechanism-based strain gradient plasticity– I. Theory, J. Mech. Phys. Solids 47 (1999) 1239–1263, http://dx.doi.org/10.1016/S0022-5096(98)00103-3.

[24] G.E. Sanoja, et al., Why is mechanical fatigue different from toughness in elastomers? The role of damage by polymer chain scission, Sci. Adv. 7 (2021) eabg9410.

[25] J. Slootman, et al., Quantifying and mapping covalent bond scission during elastomer fracture, 2020, arXiv preprint arXiv:2006.09468.

[26] J. Slootman, C.J. Yeh, P. Millereau, J. Comtet, C. Creton, A molecular interpretation of the toughness of multiple network elastomers at high temperature, Proc. Natl. Acad. Sci. 119 (2022) e2116127119.

[27] E. Zhang, R. Bai, X.P. Morelle, Z. Suo, Fatigue fracture of nearly elastic hydrogels, Soft Matter 14 (2018) 3563–3571, http://dx.doi.org/10.1039/C8SM00460A.